



Published in final edited form as:

Biochemistry. 2000 March 28; 39(12): 3206–3215.

Fetal Alz-50 Clone 1 (FAC1) Protein Interacts with the Myc-Associated Zinc Finger Protein (ZF87/MAZ) and Alters Its Transcriptional Activity[†]

K. L. Jordan-Sciutto,

Departments of Pathology and Neurobiology, University of Pittsburgh, Pittsburgh, Pennsylvania 15261

J. M. Dragich,

Departments of Pathology and Neurobiology, University of Pittsburgh, Pittsburgh, Pennsylvania 15261

J. Caltagarone,

Departments of Pathology and Neurobiology, University of Pittsburgh, Pittsburgh, Pennsylvania 15261

D. J. Hall[‡], and R. Bowser^{*}

Departments of Pathology and Neurobiology, University of Pittsburgh, Pittsburgh, Pennsylvania 15261

[‡]Department of Orthopedic Surgery, Thomas Jefferson University, Philadelphia, Pennsylvania 19107.

Abstract

Transcription factors mediate their regulatory effects through interaction with DNA and numerous nuclear proteins. The fetal Alz-50 clone 1 (FAC1) protein, a novel DNA-binding protein with the capacity to repress transcription, is likely to function through a similar mechanism (1). Using the two-hybrid yeast screen, we have shown that FAC1 interacts with the myc-associated zinc finger protein (ZF87/MAZ). This association was confirmed in vitro with recombinant protein. The ZF87/MAZ interaction domain was mapped to the region containing a putative nuclear localization signal (NLS) and nuclear export sequence (NES) of FAC1, using deletion mutants of the FAC1 protein. FAC1, on the other hand, recognizes a conformational interface that includes the proline/alanine-rich domain of ZF87/MAZ and the first zinc finger. Cotransfection of NIH3T3 cells with ZF87/MAZ and a luciferase reporter containing the SV40 promoter and enhancer results in an increase in transcriptional activation, suggesting ZF87/MAZ is able to recognize its consensus binding site present in the SV40 promoter. Cotransfection with FAC1 reduces the level of ZF87/MAZ-induced activation of the SV40 promoter in a dose dependent manner. A mutant FAC1, lacking the ZF87/MAZ interaction domain, does not alter ZF87/MAZ activation of the SV40 promoter. These data demonstrate that interaction between FAC1 and ZF87/MAZ alters the transactivation capacity of ZF87/MAZ. By immunoblot analysis, FAC1 and ZF87/MAZ exhibit similar tissue distribution and co-localize to pathologic structures in Alzheimer's disease brain. Coexpression of FAC1 and ZF87/MAZ suggest that interaction of these two proteins will have biological implications for gene regulation in neurodegeneration.

[†]This project was supported by NIH Grants: AG13208, NS10572, and AG05133.

© 2000 American Chemical Society

^{*}Address correspondence to: Department of Pathology, University of Pittsburgh School of Medicine, BST S-420, 3500 Terrace St., Pittsburgh, PA 15261. Telephone: (412) 383-7819. Fax: (412) 648-1916. bowser@np.awing.upmc.edu. .

Transcription from a given eukaryotic promoter is usually regulated by a number of DNA-binding factors. Promoter regulation is also dependent on adapter proteins as well as posttranslational modification, cooperativity, and competition between transcription factors. The fetal Alz-50 clone 1 (FAC1)¹ protein is a novel transcriptional regulator that we identified from human brain (2). It binds DNA through a unique DNA-binding motif and is able to repress transcription from a promoter containing its binding element (1). While its precise DNA-binding domain is not yet defined, FAC1 contains several other well described motifs common to transcription factors. These include the plant homeodomain/leukemia-associated protein (PHD/LAP) zinc finger motif, an acidic domain, a PEST sequence, two putative nuclear localization sequences (NLS), and a putative nuclear export sequence (NES) (3–5). In addition to these known functional domains, FAC1 has a 400 amino acid carboxyterminal domain that does not share homology with other known proteins.

The pattern of FAC1 expression and distribution within the central nervous system (CNS) suggests a functional role during neuronal development and degeneration (2, 6, 7). FAC1 protein expression levels are dramatically higher than in the adult brain, during human brain development (2). At this time, distinct patterns of FAC1 subcellular localization exist in different neuronal layers in the cortex. FAC1 localizes to the cytoplasm and neurites in less differentiated neurons located in the outer cortical layers. In more mature neurons located deeper in the cortical layers of developing brain, FAC1 is seen predominantly in the nucleus (2). Staining in the deeper cortical layers is similar to that observed in adult cortex where FAC1 protein expression is low and found predominantly in neuronal nuclei (2). These results suggest that during neuronal differentiation FAC1 is localized to the cytoplasm, while FAC1 is translocated to the nucleus upon terminal differentiation. This pattern of expression and subcellular distribution is also observed in motor neurons during spinal cord development and in murine brain development (6, *and unpublished observations*). Finally, FAC1 protein distribution also changes during an in vitro model of neuronal differentiation. In untreated PC12 cells, FAC1 is found in the nucleus and surrounding the nuclear membrane. Upon treatment with NGF, FAC1 localizes to the cytoplasm and extending neurites of PC12 cells (Rhodes, J., and Bowser, R., unpublished observations). These observations suggest that developmental stimuli regulate subcellular distribution of FAC1.

FAC1 expression levels and subcellular localization also change during neurodegeneration associated with Alzheimer's disease (AD) and amyotrophic lateral sclerosis (ALS) (6, 7). In contrast to the nuclear localization observed in adult neurons, FAC1 becomes localized throughout the nucleus, cell body, and neurites in areas associated with disease pathology (2, 6, 7). In the case of Alzheimer's disease, FAC1 co-localizes with one of the hallmark pathologic features, the β -amyloid plaque (7). FAC1 is also found in dystrophic neurites and Hirano bodies, both of which are prevalent in Alzheimer's disease (8). In unaffected adjacent neurons, FAC1 retains its nuclear localization, suggesting that changes in FAC1 are in response to the degenerative stimuli. Such degenerative stimuli include accumulation of insoluble β -amyloid (reviewed in 9). Treatment of NGF-differentiated PC12 cells with aggregated β -amyloid results in altered FAC1 subcellular localization. Again, FAC1 leaves the nucleus and localizes to the cell body and neurites (Rhodes, J., and Bowser, R., unpublished observations). Similarly, FAC1 protein expression is elevated in motor neurons and exhibits altered subcellular localization in ALS (6). These data support a re-expression and redistribution of FAC1 protein in response to degenerative stimuli.

¹Abbreviations: Alzheimer's disease, AD; amyotrophic lateral sclerosis, ALS; central nervous system, CNS; cytomegalovirus, CMV; Dulbecco's modified essential media, DMEM; enhanced chemiluminescence, ECL; fetal Alz-50 clone 1, FAC1; glutathione-S-transferase, GST; hemagglutinin, HA; horseradish peroxidase, HRP; in vitro translated, IVT; Myc-associated zinc finger protein, ZF87/MAZ; nuclear export signal, NES; nuclear localization signal, NLS; phosphate-buffered saline, PBS; plant homeodomain/leukemia-associated protein, PHD/LAP; simian virus-40, SV40; sodium dodecyl sulfate polyacrylamide gel electrophoresis, SDS-PAGE; Tris-buffered saline, TBS.

In addition to neuronal differentiation and degeneration, FAC1 also exhibits altered subcellular localization in a model for neuronal regeneration. In a rat brain entorhinal cortex lesion model, FAC1 expression rapidly increases in the denervated area by 2 days post lesion (10). At 6 days post lesion, FAC1 immunoreactivity is found in the cytoplasm and dendrites, extending through the denervated outer molecular layer. At 30 days post lesion, FAC1 immunoreactivity has returned to the nuclei of surviving neurons. These observations support a role for FAC1 in neuronal regeneration.

The similarity in the behavior of the FAC1 protein during three distinct neuronal responses suggests a connection between these processes. To understand the role of FAC1 in these neuronal conditions, we need to determine the function of FAC1 and how this function is regulated. Nuclear localization of FAC1 is consistent with our previously defined role for FAC1 as a transcriptional regulator. Changes in FAC1 subcellular localization are one mechanism by which FAC1 transcriptional activity may be regulated. FAC1 transcriptional efficacy may be further regulated through interactions with other transcription factors. To test if FAC1 function is regulated by such mechanisms, we used the two-hybrid yeast screen to identify potential interacting proteins from a human fetal brain cDNA library. We identified an interaction with the myc-associated zinc finger protein (ZF87/MAZ), which was confirmed by several other experimental methods. This interaction was found to have a functional consequence on ZF87/MAZ transcriptional regulation. FAC1 reduces promoter activity induced by ZF87/MAZ in cultured fibroblasts. FAC1 and ZF87/MAZ expression correlate in various tissues and brain regions. These data suggest that FAC1 can interact with ZF87/MAZ in a biological context and alter its function as a transcription factor.

EXPERIMENTAL PROCEDURES

Two-hybrid Yeast Screen. Strains and Media

The strain of *Saccharomyces cerevisiae* used for the two-hybrid yeast screen was previously described by Vojtek et al. (11). The reporter strain used was L40 (MAT_a, trp1, leu2, LYS2::lexA-HIS3, URA3::lexA-lacZ (Sternglanz, Weintraub, and Hollenburg, unpublished data). Yeast cells were grown in rich media YPD_A (1% yeast extract, 2% bacto-peptone, 2% glucose, and 0.1 μ g/mL adenine) or in synthetic media, lacking amino acids for which the yeast cells are auxotrophic due to the presence of a particular plasmid marker.

Plasmids

The LexA:FAC1(438–810) plasmid encoded amino acids 438–810 of the human FAC1 cDNA. This sequence was cloned in frame with the LexA coding sequence in plasmid pBTM116 (12, 13). For bait, a human fetal brain cDNA library was constructed in the plasmid pACT2 (Clontech). PACT2 is a high copy yeast vector, which contains the coding region for the transcriptional activation domain of the herpes virus VP16 transactivator as well as the LEU2 marker gene coding for a gene product needed for leucine biosynthesis (11).

Library Screen

The screen was performed as previously described by Jordan et al. (14). L40 cells were transformed with LexA:FAC1(438–810) (The yeast strain was a kind gift from Stan Hollenberg, and the pBTM116 plasmid used to make LexA:FAC1(438–810) was constructed by Paul Bartel and Stanley Fields). The plasmid was maintained by auxotrophy for the TRP1 marker. L40 containing LexA:FAC1(438–810) was then prepared for electroporation of the library. A 200 μ g sample of the human fetal brain cDNA library in the pACT2 plasmid (Clontech) was electroporated into 50 μ L aliquots of L40 containing pLexA-FAC1(438–810). Electroporated cells were plated onto media lacking Ura, Lys, Trp,

Leu, and His. Growth on His(-) plates indicates that an interaction between FAC1(438–810) and the protein coded by the unknown cDNA. Colonies were then assayed for β -galactosidase activity to ensure that the interaction between FAC1(438–810) and the protein coded by the unknown cDNA was not specific for the heterologous promoter driving HIS3 gene expression. The pACT2 plasmid containing the unknown cDNA was then isolated by the “smash and grab” method (11), and the cDNA insert was sequenced.

GST Fusion Affinity Column Chromatography

cDNA's coding for FAC1(438–810), FAC1(610–810), FAC1(700–762), FAC1(700–782), FAC1(738–762), FAC1(738–782), ZF87/MAZ, ZF87/MAZ(1–125), ZF87/MAZ(1–255), ZF87/MAZ(197–298), and ZF87/MAZ(298–423) were cloned into pGEX-5x-1 (Pharmacia) in frame with the glutathione-S-transferase gene (GST). Fusion proteins were produced as previously described (15). Briefly, the proteins were induced with IPTG for 3 h, bacteria were lysed, and then the protein was separated from cellular debris by centrifugation. The GST fusion proteins were purified by the specific interaction between GST and glutathione immobilized on sepharose beads (Pharmacia), using the bacterial extracts. At this point, the protein:sepharose column was used as an affinity column for the fusion protein it contained.

In Vitro Transcription/Translation

In vitro transcription reactions were performed by cloning FAC1(438–810) into the *EcoRI* site of pBluescript II KS+. An initiator methionine sequence was cloned into the *HindIII* site for translation initiation. ZF87/MAZ was cloned into pcDNA3.1+, which contains a T7 promoter at the 5' end. The constructs were linearized, and RNA was generated using purified T3 polymerase for FAC1 and T7 polymerase for MAZ. The mRNA transcripts (315–325 ng) were used to generate the ³⁵S-labeled FAC1(438–810) and ZF87/MAZ proteins using an in vitro translation reaction with a nuclease treated rabbit reticulocyte lysate (35 μ L, Promega) in a total reaction volume of 50 μ L. ³⁵S-methionine at 0.9 mCi/mL was also included in the reactions.

Cellular Protein Extracts for GST-pulldown Assay

Protein extracts were prepared from epitope-tagged ZF87/MAZ transfected PT67 cells by detergent lysis on ice (0.1% NP-40, 10 mM Tris (pH 8.0), 10 mM MgCl₂, 15 mM NaCl, 0.5 mM PMSF, 2 μ g/mL Pepstatin A, and 1 μ g/mL leupeptin) (16). The nuclei were collected by low-speed centrifugation at 800 *g* for 5 min. The supernatant was saved as the “cytosolic extract”, and the pellet containing the nuclei were further extracted with high salt buffer (0.42 M NaCl, 20 mM Hepes (pH 7.9), 20% glycerol, 0.5mM PMSF, 2 μ g/mL pepstatin A, and 1 μ g/mL leupeptin) on ice for 10 min. Residual insoluble material was removed by centrifugation at 14000*g* for 5 min. The supernatant fraction was collected and termed the “nuclear extract”. Protein concentrations were determined by Biorad protein assay.

GST-pulldown Assays

In vitro transcribed and translated protein or 500 μ g of nuclear protein extracts transfected with epitope-tagged ZF87/MAZ were added to GST affinity columns in binding buffer (150 mM NaCl, 20 mM Tris (pH 8), 1 mM EDTA (pH 8.0), 125 mM PMSF, 2 μ g/mL pepstatin A, 1 μ g/mL benzamidine, and 1 μ g/mL leupeptin). The affinity columns were then washed five times with 10 bed volumes of NETN (150 mM NaCl, 20 mM Tris (pH 8), 1 mM EDTA, 0.5% NP40, 125 mM PMSF, 2 μ g/mL pepstatin A, and 1 μ g/mL leupeptin). Proteins retained on the column were eluted by boiling the columns in SDS-PAGE sample buffer. The eluted proteins were then electrophoresed on a 10% SDS polyacrylamide gel. For the in vitro translated proteins, the gels were dried and exposed to X-ray film. For gels containing protein extracts, see immunoblotting protocol.

Immunoblotting

The proteins were transferred from the SDS-PAGE to nitrocellulose by electrophoresis and blocked in 5% nonfat milk TBS (10 mM Tris (pH 8.0), 150 mM NaCl). Monoclonal M2 antibody (Kodak, IBI) and the polyclonal HA antibody (Santa Cruz) were used at 1:1000 in 0.5% milk overnight at 4 °C. The monoclonal FA-1 antibody, which recognizes the FAC1 protein, was used at 1:10 in 5% milk overnight at 4 °C. A polyclonal antibody against ZF87/MAZ was used at 1:1000 in 5% milk overnight at 4 °C. Blots were washed three times in TBS for 15 min. An isotype specific secondary antibody was used to detect M2 and FA-1 (goat anti-mouse IgG1-HRP, 1:500, Jackson Laboratories), and goat anti-rabbit HRP(1:500, Jackson Laboratories) was used to detect the HA antibody and the anti-ZF87/MAZ antibody. The secondary antibody was washed extensively in TBS, three times for 20 min. The antibody was then visualized using enhanced chemiluminescence (ECL) (Renaissance, NEN life Science Products, Inc.)

Co-immunoprecipitation

PT67 cells were transfected with M2-tagged FAC1 and HA-tagged ZF87/MAZ. 800 μg of nuclear protein extracts made from these cells was incubated with 15 μL of M2-agarosebeads (Sigma) in 150 mM NaCl, 20 mM Hepes (pH 7.9), 20% glycerol, 0.5 mM PMSF, 2 $\mu\text{g}/\text{mL}$ pepstatinA, and 1 $\mu\text{g}/\text{mL}$ leupeptin for 4 h at 4 °C. The beads were collected by centrifugation, and the unbound proteins in the supernatant were reserved. A fourth of the supernatant was loaded onto the SDS-PAGE gel (see below). The beads were washed 5 times with NETN (see GST pull down assay). Proteins bound to the beads were eluted by boiling in 1X SDS sample buffer. The beads were pelleted, and the supernatant was run on an 8% SDS-PAGE along with 300 μg of PT67 nuclear extracts used as starting material and 1/4 of the volume of the unbound protein fraction. The gel was transferred to nitrocellulose and immunoblotted.

Cell Culture and Transient Transfection via Calcium Phosphate

NIH3T3 mouse fibroblasts were cultured in Dulbecco's modified essential media (DMEM) containing 10% bovine serum. PT67 cells, a retroviral packaging cell line based on NIH3T3 cells, were cultured in DMEM containing 10% fetal bovine serum. The media was changed every 3 days and the cells were split 1:5 once they came in contact with each other. Cells were plated at a density of 25 000 cells/mL. Transient transfections were initiated on tissue culture dishes that were 20–50% confluent (12).

Transfection DNA was resuspended in a 250 mM CaCl_2 solution that was added dropwise to a 2X Hepes buffered saline solution (Profection, Promega). The resulting mixture was allowed to precipitate for 20 min prior to addition to cells. Four hours after addition of DNA, the NIH3T3 cells were glycerol shocked for two minutes with 10% glycerol DMEM. Plates were washed 3X with PBS and fresh media was added. For PT67 cells, the media was replaced with fresh media 24 h posttransfection. This was found to give the best transfection efficiency.

Cells were harvested 48 h after transfection. *Photinus* luciferase production was assayed by scraping cells in luciferase assay lysis buffer, vortexing, removing the cellular debris by centrifugation, and collecting the supernatant; 20 μL of supernatant solution was added to 75 μL luciferase reagent (Promega) and measured in a luminometer (Berthold lumomat LB9501). Luminescence values were normalized to protein concentration as determined by Biorad Protein Assay. Each transfection was performed a total of three times. The standard deviation was below 0.1%, suggesting that the transfection efficiencies were similar for each reaction.

Tissue Samples and Microscopy

The midfrontal cortex from six cases of clinically diagnosed AD, and six nondemented age-matched controls were utilized to examine protein expression and distribution. The average age at death was 82 years for AD cases (range 76–90 years) and 64 years (range 52–75) for control cases. Neuropathologic examination to identify senile plaques and neurofibrillary tangles was performed for all cases at the time of autopsy to confirm the diagnosis of AD using CERAD criteria. Approval for use of human tissues was obtained from the University of Pittsburgh Interval Review Board. For immunoblot analysis, fresh frozen tissue samples were homogenized in lysis buffer and utilized as previously described (5). For immunohistochemistry, all tissue was fixed in 10% buffered formalin for 1 week. 40 μm Vibratome or cryostat sections were examined as follows.

For light microscopy, tissue sections were incubated in 3% H_2O_2 + 0.25% Triton X-100 in PBS (phosphate-buffered saline) for 30 min. The sections were then blocked in 5% milk/PBS for 1 h. Primary antibody (1:400 dilution) was added in 0.5% milk/PBS and incubated overnight at 4 °C. After four washes in PBS, sections were incubated in biotinylated goat anti-rabbit IgG secondary antibody (1:1000 dilution) for 1.5 h. Upon washing, the sections were incubated in streptavidin–HRP (1:1000 dilution) for 1 h and the reaction product visualized with diaminobenzidine (DAB).

For confocal laser microscopy, tissue sections were first treated with 3% H_2O_2 + 0.25% TX-100 for 30 min and blocked in 5% milk/PBS for 1 h at RT. Anti-ZF87/MAZ (1:400 dilution) and/or anti-phospho-FAC1 antibodies (FA2 at 1:10 dilution) were added and the sections incubated overnight at 4 °C. After PBS washes, the sections labeled with anti-FAC1 antibody were incubated in biotinylated goat anti-mouse IgG1 (1:500) for 2 h and washed in PBS. Sections labeled with the FAC1 antibody were then incubated with a 1:500 dilution of streptavidin–Cy5. Sections labeled with the Anti-ZF87/MAZ antibody were incubated with 1:500 dilution of goat anti-rabbit–FITC (1:500 dilution, Jackson ImmunoResearch Labs, Inc., West Grove, PA) for 1.5 h at room temperature. After PBS washes, the sections were analyzed on a Molecular Dynamics Model 2001 laser scanning confocal microscope. Omission of the primary antibody resulted in absence of fluorescent signal. Crossover control experiments were also performed for each primary antibody against the secondary antibody from the other label in order to determine the specificity of the secondary antibody.

RESULTS

FAC1 interacts with the myc-associated zinc finger protein (ZF87/MAZ)

FAC1 is a transcriptional repressor that exhibits altered subcellular distribution during development. Since both these attributes can be regulated through protein–protein interaction, we hypothesize that FAC1 function is regulated by interaction with other cellular proteins. We have previously shown that numerous cellular proteins from human fetal brain extracts associate with FAC1 via affinity chromatography (2). To identify cellular proteins that interact with FAC1 and may be involved in regulating FAC1 function, we performed a two-hybrid yeast screen (11, 14). This screen identifies interactions between a protein of interest fused to a DNA-binding domain and an unknown protein encoded by a human fetal brain cDNA library fused to an acidic activation domain. If the two fusion proteins interact, then the acidic domain and DNA-binding domain are brought into the same vicinity. This complex now has the capacity to activate promoters containing the consensus site for the DNA-binding domain. The binding site, in our case, the LexA-binding site, is found in the promoter regions of the HIS3 gene, which encodes a protein required for histidine synthesis and the LacZ gene, which can be assayed by a colorimetric assay. Two FAC1 domains were tested for use in the screen: the C-terminal domain (amino acids 438–

810) and N-terminal domain (amino acids 1–398). The N-terminal domain could not be used as it generated a high level of false positives (histidine synthesizing yeast in absence of a cDNA containing library vector; data not shown). The acidic region in the N-terminal domain most likely acts to recruit endogenous yeast RNA polymerase to the promoter and initiate transcription. The C-terminal domain did not produce a high level of false positives and was pursued in the screen with a human fetal brain cDNA library (Figure 1, VP16 alone). Of the 8×10^5 colonies screened, 88 were positive for histidine synthesis, suggesting an interaction between FAC1(438–810) and the protein produced by the cDNA present in the library vector. These 88 were subjected to a secondary screen for LacZ expression; 44 clones were LACZ positive and pursued further. To confirm that the 44 positive clones encoded true interacting proteins, the plasmids were isolated from yeast colonies, transformed into bacteria, and reintroduced into freshly grown yeast with LexA:FAC1(438–810) and tested for histidine auxotrophy. The library vectors were also introduced by themselves into yeast to ensure that the proteins they encoded were not activating transcription by directly binding the promoter bypassing interaction with the LexA:FAC1(438–810) fusion protein. Of the 44 remaining clones, only 11 passed these final rounds of screening. These 11 clones were sequenced and compared to Genbank and found to contain five unique sequences. Four of these await further investigation. The fifth sequence encoded the myc-associated zinc finger protein, ZF87/MAZ, which forms the basis of the current study. Figure 1 demonstrates that yeast containing both LexA:FAC1(438–810) and VP16:MAZ grow on plates lacking histidine, suggesting an interaction between FAC1 and ZF87/MAZ, which brings the VP16 activation domain into the vicinity of the LexA DNA-binding domain and induces expression of the HIS3 gene product. As a negative control, LexA:FAC1(438–810) is introduced with pACT2, which expresses the VP16 activation domain (VP16) to show that the interaction is due to the presence of the ZF87/MAZ polypeptide. These data suggest that FAC1 interacts with the ZF87/MAZ protein when coexpressed in yeast.

ZF87/MAZ Interacts Optimally with a Region of FAC1 Containing a Putative Nuclear Localization Sequence (NLS) and the Nuclear Export Sequence (NES)

To demonstrate a specific interaction between FAC1 and ZF87/MAZ, we used a panel of FAC1 mutants in the GST pull-down assay. In vitro translated (IVT) ZF87/MAZ was incubated with affinity columns containing various GST:FAC1 fusion proteins (Figure 2A). The GST:FAC1 fusion proteins include specific functional domains to identify motifs that contribute to interaction with ZF87/MAZ. The same amount of IVT ZF87/MAZ was loaded onto each column and loaded onto the first lane of the gel (Figure 2B, lane 1). As a negative control, GST alone does not bind IVT ZF87/MAZ (Figure 2B, lane 2). GST:FAC1(611–810) retains maximum ZF87/MAZ binding activity (Figure 2B, lane 3). GST:FAC1(438–610), which contains the PEST sequence, had no affinity for ZF87/MAZ (data not shown). GST:FAC1(611–750) contains only the putative NLS and does not bind ZF87/MAZ optimally (Figure 2B, lane 4). GST:FAC1(700–762) contains the putative NLS, but not the predicted NES region, and has the same binding as the previous construct (Figure 2C), suggesting amino acids 700–750 are responsible for the observed but reduced ZF87/MAZ binding (Figure 2B, lane 5). GST:FAC1(700–782) encodes both the putative NLS and NES and binds ZF87/MAZ as avidly as the larger construct, suggesting this sequence is responsible for ZF87/MAZ binding (Figure 2B, lane 6 and 8; and Figure 2C). GST:FAC1(738–762) contains the sequence between the predicted NLS and the NES and does not bind ZF87/MAZ at all, suggesting it does not contribute to the interaction (Figure 2B, lane 7). GST:FAC1(738–782) encodes the putative NES, which also binds ZF87/MAZ (Figure 2, lane 8 vs lane 6); however, it binds 3-fold less protein than the constructs containing both the NLS and NES (Figure 2C, 738–782 and 700–782). Each of the fusion proteins were present on the columns in excess as verified by Ponceau S staining of the

proteins on the nitrocellulose (data not shown). These data were quantified using NIH image 1.5.8 software and displayed as a bar graph in Figure 2C. The quantification shows that amino acids 700–782 of FAC1 bind ZF87/MAZ as well as amino acids 610–810, but the other constructs containing either the NLS alone or the NES alone bind 3-fold less ZF87/MAZ. These data suggest that ZF87/MAZ interacts with FAC1 as it has affinity for defined regions of the protein, and ZF87/MAZ interacts with the domain containing the putative NLS and NES sequences present in FAC1. This interaction site on FAC1 suggests ZF87/MAZ may play a role in regulating FAC1 localization after transport to the nucleus.

FAC1 Interacts with ZF87/MAZ

To further support our findings that FAC1 interacts with ZF87/MAZ, we did the reverse experiment. Various GST:ZF87/MAZ affinity columns were made (shown in Figure 3A) and incubated with IVT FAC1(438–810) (input; Figure B, lane 1). GST alone was included as a negative control and indeed FAC1(438–810) does not interact with GST (Figure 3B, lane 2). FAC1 does interact with full-length ZF87/MAZ (Figure 3B, lane 3), further confirming the observations in the two-hybrid screen and Figure 2. FAC1 interacts with the amino terminal domain of ZF87/MAZ (Figure 3B, lane 4 and 5), which is proline- and alanine-rich and does not contain the zinc fingers. FAC1 also appears to have reduced affinity for the peptide containing amino acids 197–298 of ZF87/MAZ (Figure 3B, lane 6). This may be due to overlap between this construct and the one containing amino acids 1–255 (Figure 3A), or may be due to the presence of the first zinc finger. FAC1 does not have substantial affinity for the five carboxy-terminal zinc fingers of ZF87/MAZ (Figure 3B, lane 7), which are responsible for DNA binding activity. However, quantification of FAC1(438–810) bound by each of the ZF87/MAZ deletion constructs indicates that none of the ZF87/MAZ deletion constructs bind FAC1 as well as the full-length protein (Figure 3C). This was not due to differences in the amount of fusion protein present on the columns, which was verified by Ponceau S staining to be in excess (data not shown). This suggests that the interaction may involve a conformational interaction interface that requires multiple regions of the ZF87/MAZ protein. However, the interaction does not require the zinc fingers of FAC1, eliminating the possibility that the observed association is due to nonspecific interaction between the zinc finger domains often observed in an *in vitro* assay. While zinc finger domains are the basis for many protein:protein interactions (4, 5), in this case, the interaction appears to be independent of the respective zinc finger domains of each protein.

In Vivo Produced ZF87/MAZ Interacts with FAC1

To further confirm FAC1 interaction with ZF87/MAZ, PT67 cells were transiently transfected with epitope-tagged ZF87/MAZ under control of the cytomegalovirus (CMV) promoter. Nuclear extracts from these cells, which contain the epitope-tagged ZF87/MAZ (Figure 4A, lane 1) were incubated with GST:FAC1 affinity columns. GST alone did not bind ZF87/MAZ (Figure 4A, lane 2) and neither did GST:FAC1(401–500), which contains the PEST domain (Figure 4A, lane 3). GST:FAC1(611–810) binds ZF87/MAZ (Figure 4A, lane 4), which is consistent with the data presented in Figure 2. This suggests that FAC1 can recognize ZF87/MAZ in the presence of other mammalian nuclear factors, suggesting that this interaction is specific. To demonstrate that FAC1 and ZF87/MAZ interact *in vivo*, we cotransfected PT67 cells with M2-tagged FAC1 and hemagglutinin (HA) tagged ZF87/MAZ. We precipitated M2-FAC1 from 800 μ g of PT67 M2-FAC1:HA-ZF87/MAZ nuclear extracts in 150 mM NaCl binding buffer, using agarose bound M2 antibody. Proteins bound to the M2 column were fractionated by SDS-PAGE, transferred to nitrocellulose and visualized using the HA antibody (Figure 4B, lane 2). Approximately 10% of the HA-tagged ZF87/MAZ is retained on the column as compared to the amount of protein input (Figure 4B, lane 1) and the amount retained in the unbound supernatant (Figure 4B, lane 3). This suggests that ZF87/MAZ produced in mammalian cells associates with M2-FAC1. Two

additional proteins are bound by the M2-FAC1 column and recognized by the HA antibody. The 55 kD protein in the M2 lane is most likely the M2 antibody heavy chain, explaining both its presence and abundance. The 100 kD band in the same lane is an unknown protein bound by M2 and recognized by the HA antibody. Its presence in the M2 lane alone suggests that it is also a product of the M2-agarose beads.

FAC1 Reduces Transcriptional Activation by ZF87/MAZ

ZF87/MAZ has been shown to have various effects on transcription. It can act as an activator or a repressor depending on the promoter context and cell background being used. In NIH3T3 cells (Figure 5A), ZF87/MAZ is a potent activator of the SV40 promoter (Figure 5A, compare – and + ZF87/MAZ). ZF87/MAZ activation of this promoter is likely occurring through the characterized SP1 binding sites found in the SV40 promoter (17). ZF87/MAZ has been shown to recognize SP1 binding sites in several promoter contexts (18–20). Transfection of NIH3T3 cells with the SV40 promoter and FAC1 has no effect on transactivation of the luciferase reporter, since there are no FAC1 binding elements in the SV40 promoter (Figure 5A). However, cotransfection of ZF87/MAZ with increasing concentrations of full-length FAC1 results in a dose dependent decrease in ZF87/MAZ transactivation (Figure 5A). Mutant FAC1 lacking the ZF87/MAZ interaction domain, but containing the amino-terminal NLS, exerts no effect on ZF87/MAZ activity (Figure 5B) nor does it affect expression from the SV40 promoter by itself (Figure 5B). ZF87/MAZ, FAC1-FL, and FAC1(1–398) are expressed at comparable levels in cotransfected NIH3T3 cells, so the observed effects are not due to differences of protein expression from the CMV promoter (data not shown). These data demonstrate that the presence of FAC1 represses ZF87/MAZ function in these cells. This repression requires interaction between ZF87/MAZ and FAC1, because removal of the carboxy-terminal domain that interacts with ZF87/MAZ eliminates the repressive effect on transcriptional activity exerted by the full-length protein. Therefore, ZF87/MAZ activity is regulated by interaction with FAC1.

ZF87/MAZ and FAC1 Exhibit Similar Patterns of Expression in Various Tissues and Alzheimer's Disease

For an interaction between two proteins to have a functional and physiological consequence, they must be expressed in the same cell. To address this issue, we assayed for the presence of both FAC1 and ZF87/MAZ in several tissue types and various brain regions by immunoblot analysis. When normalized for sample loading, both ZF87/MAZ and FAC1 exhibit highest expression in liver and kidney, and lowest in heart and small intestine (Figure 6 A). Although FAC1 and ZF87/MAZ are expressed in the same tissues, the ratio of ZF87/MAZ to FAC1 varies among those tissues (Figure 6C). This is in contrast to what we observed when we looked at expression in various brain regions. Expression levels of FAC1 and ZF87/MAZ were highest in midfrontal cortex and motor cortex (Figure 6B). Across all the brain regions tested the relative amount of FAC1 correlated with the relative amount of ZF87/MAZ (Figure 6D). These data confirm that FAC1 and ZF87/MAZ exhibit a similar tissue distribution. Since both FAC1 and ZF87/MAZ are expressed in midfrontal cortex, we assayed ZF87/MAZ cellular localization in this region. We observed low level ZF87/MAZ staining in the midfrontal cortex, using immunohistochemistry. Cells staining positive for ZF87/MAZ exhibited morphology suggestive of neurons (Figure 7A). This is consistent with staining for FAC1 also being predominantly in neurons; however, the subcellular localization appears distinct (Figure 7A and (2)). While FAC1 is found predominantly in nuclei of neurons, ZF87/MAZ exhibits a more diffuse staining of neuronal cell bodies. This suggests that FAC1 and ZF87/MAZ are present in the same cells, but exhibit distinct subcellular localization in normal, aged adult brain. In midfrontal cortex from an Alzheimer's disease patient ZF87/MAZ staining localizes to plaque like structures, which is consistent with FAC1 staining (Figure 7, B and C). To confirm that FAC1 and ZF87/MAZ

co-localize during Alzheimer's disease, we did double-labelled immunofluorescent laser confocal microscopy for FAC1 and ZF87/MAZ. FAC1 and ZF87/MAZ co-localize to plaque like structures. An example of a plaque positively labeling for FAC1 (red) and ZF87/MAZ (green) is shown in Figure 7, D and E. These data demonstrate that ZF87/MAZ exhibits a pattern of expression and localization similar to FAC1 during neurodegeneration associated with Alzheimer's disease.

DISCUSSION

We have identified ZF87/MAZ as a binding partner for the FAC1 protein, using the two-hybrid yeast screen. This interaction was confirmed by GST pull-down assays, using both in vitro and in vivo produced ZF87/MAZ and by co-immunoprecipitation. Further, we have demonstrated that ZF87/MAZ specifically interacts with the domain containing the putative NLS and NES motifs found in the carboxy-terminal domain of FAC1. Conversely, FAC1 requires the first 297 amino acids of ZF87/MAZ protein indicating that FAC1 may bind an interface created by a specific conformation induced by the tertiary structure of ZF87/MAZ. The identification of the interaction domains is important because both proteins recognize motifs apart from the DNA-binding domain of the binding partner, suggesting that both proteins may retain the ability to bind DNA when in association with each other. ZF87/MAZ interaction with the domain containing the NLS/NES of FAC1 also suggests it may act as a regulator of FAC1 retention in the nucleus of cells or vice versa. Because FAC1 exits the nucleus in response to neuronal degenerative stimuli (6, 7), determining how the interaction between FAC1 and ZF87/MAZ is regulated will be important for understanding the role of both proteins in neurodegenerative disease progression. ZF87/MAZ has been shown to compete for promoter site binding with other G/C-rich binding proteins such as SP1, SP3, and YY1 (20). The relative abundance and DNA binding affinity of these proteins is proposed to determine cell type specific promoter activity (20). Here, we demonstrate an additional level of control that can be exerted through G/C-rich promoter elements. To address the functional consequence of interaction between these two proteins, we assessed the ability of ZF87/MAZ to activate transcription of the SV40 promoter and the consequence of adding FAC1. ZF87/MAZ causes a dramatic increase in expression from the SV40 promoter in NIH3T3 cells likely through the G/C-rich SP1 binding sites already characterized (17–20). Activation by ZF87/MAZ is reduced in a dose dependent manner by the presence of FAC1. This suggests that the function of the interaction between ZF87/MAZ and FAC1 is to fine-tune or modulate expression of genes containing G/C-rich elements in diverse cell types and cell responses. According to the literature, ZF87/MAZ exhibits promoter specific as well as cell type specific transcriptional activity. For example, ZF87/MAZ acts as an activator of the insulin promoter in HeLa cells and an insulinoma cell line (21), but represses activation of the c-myc P2 promoter in Cos cells (22). Numerous rationales for this variation in ZF87/MAZ activity have been proposed in the literature (18, 20, 22–24). As an additional form of regulation, we show here that association of ZF87/MAZ with other proteins, namely, FAC1, modulates its activity. Modulation of ZF87/MAZ activity by FAC1 is possible in several tissues including the kidney and midfrontal cortex. Further, we have shown that FAC1 and ZF87/MAZ co-localize with each other in areas associated with the pathology of Alzheimer's disease. ZF87/MAZ proteins are present not only in the same tissues but also in FAC1 positive cells, according to experiments performed by others demonstrating ZF87/MAZ repressor activity. For example, in Neuro2A cells, ZF87/MAZ competes with SP1 for promoter element binding and acts as a transcriptional repressor for phenylethanolamine *N*-methyltransferase gene (20). ZF87/MAZ also represses transcription of the c-myc promoter in Cos cells (22). Both Cos cells and cells of neuronal origin express abundant quantities of FAC1 (1). Here, we have shown that ZF87/MAZ acts as an activator in NIH3T3 cells, which express low if any FAC1. We suggest that the presence of FAC1 is one mechanism that accounts for altered function of ZF87/MAZ in

FAC1 expressing cells. The presence of both FAC1 and ZF87/MAZ in areas of AD pathology suggests these two proteins may play a role in AD progression. A number of genes implicated in AD contain both putative FAC1- and ZF87/MAZ-binding elements in their 5' regulatory regions including the APP promoter, Presenilin-1, and Cu²⁺/Zn²⁺ superoxide dismutase-1 (25–27). Our data suggests that these promoters may be regulated by interaction of these two DNA-binding proteins. Future experiments will be aimed at determining if FAC1 and ZF87/MAZ interact when bound to their cognate sites in a promoter. ZF87/MAZ has been shown to induce a 72° bend in the DNA (28). Further, others have shown that ZF87/MAZ plays a structural role in CD4 promoter function (23, 28). Together these findings suggest that under normal cellular conditions, interactions between FAC1 and ZF87/MAZ may alter the structure of transcriptional regulatory regions containing their cognate binding sites. Changes in the functional interactions between these two proteins may contribute to progression of AD.

Both FAC1 and ZF87/MAZ are expressed in the various brain regions. Our previous studies implicate FAC1 in the process of neuronal development as well as degeneration. Others have found that ZF87/MAZ also exhibits altered activity during neuronal differentiation (2, 29, 30). Transactivation by ZF87/MAZ was decreased, using the c-myc promoter to gauge ZF87/MAZ activity, during the first 24 h of differentiation, returned to normal by 48 h, and reduced again at 96 h (29). This is similar to the time frame in which we see changes in FAC1 subcellular distribution in differentiating PC12 cells (Rhodes, J., and Bowser, R., unpublished observations). Interaction between ZF87/MAZ and FAC1 further implicates ZF87/MAZ in other neuronal processes. The interaction between FAC1 and ZF87/MAZ suggests the following model for gene regulation during these important neuronal processes. We propose that in response to degenerative, regenerative, or developmental stimuli, the subcellular localization of FAC1 changes from nuclear to cytoplasmic. When this occurs, ZF87/MAZ activity also changes. This results in altered expression of numerous genes containing G/C-rich promoter sequences including the ZF87/MAZ promoter itself (31). Understanding the regulation and function of the interaction between FAC1 and ZF87/MAZ will provide insight into molecular mechanisms underlying neuronal responses to both developmental and degenerative stimuli.

Acknowledgments

We would like to thank Dr. Joseph Locker for experimental advice and Aryn Gettis and Lazarus Vojanovic for technical support.

REFERENCES

1. Jordan-Sciotto K, Dragich J, Rhodes J, Bowser R. J. Biol. Chem. 1999; 274:35262–35268. [PubMed: 10575013]
2. Bowser R, Giambone A, Davies P. Dev. Neurosci. 1995; 17:20–37. [PubMed: 7621746]
3. Zhu P, Bowser R. Biochim. Biophys. Acta. 1996; 1309:5–8. [PubMed: 8950167]
4. Saha V, Chaplin T, Gregorini A, Ayton P, Young B. Proc. Nat. Acad. Sci. U.S.A. 1995; 92:9737–9741.
5. Aasland R, Gibson TJ, Stewart AF. Trends Biochem. Sci. 1995; 20:56–59. [PubMed: 7701562]
6. Mu X, Springer JE, Bowser R. Exp. Neurol. 1997; 146:17–24. [PubMed: 9225734]
7. Schoonover S, Davies P, Bowser R. J. Neuropathol. Exp. Neurol. 1996; 55:444–455. [PubMed: 8786404]
8. Jordan-Sciotto K, Dragich J, Walcott D, Bowser R. Neuropathol. App. Neurobiol. 1998; 24:359–366.
9. Selkoe D. Nature. 1999; 399:A23–A31. [PubMed: 10392577]
10. Styren SD, Bowser R, DeKosky ST. J. Comp. Neurol. 1996; 386:555–561. [PubMed: 9378851]

11. Vojtec A, Hollenberg S, Cooper J. *Cell*. 1993; 74:205–214. [PubMed: 8334704]
12. Fields S, Song O. *Nature*. 1989; 340:245–246. [PubMed: 2547163]
13. Chien C-T, Bartel PL, Sternglanz R, Fields S. *Proc. Nat. Acad. Sci. U.S.A.* 1991; 88:9578–9582.
14. Jordan KL, Evans DL, Steelman S, Hall DJ. *Biochemistry*. 1996; 35:12320–12328. [PubMed: 8823166]
15. Jordan KL, Haas AR, Logan TJ, Hall DJ. *Oncogene*. 1994; 9:1177–1185. [PubMed: 8134120]
16. Logan T, Jordan K, Evans D, Hall D. *J. Cell. Biochem*. 1997; 64:1–12.
17. Dynan W, Tjian R. *Cell*. 1983; 35:79–87. [PubMed: 6313230]
18. Parks C, Shenk T. *J. Biol. Chem*. 1996; 271:4417–4430. [PubMed: 8626793]
19. Karantzoulis-Fegaras F, Antoniou H, Lai S-LM, Kulkarni G, D'Abreo C, Wong G, Miller T, Chan Y, Atkins J, Wang Y, Marsden P. *J. Biol. Chem*. 1999; 274:3076–3093. [PubMed: 9915847]
20. Her S, Bell R, Bloom A, Siddall B, Wong D. *J. Biol. Chem*. 1999; 274:8698–8707. [PubMed: 10085109]
21. Kennedy G, Rutter W. *Proc. Natl. Acad. Sci. U.S.A.* 1992; 89:11498–11502. [PubMed: 1454839]
22. Izzo M, Strachan G, Stubbs M, Hall D. *J. Biol. Chem*. 1999; 274:19498–19456. [PubMed: 10383467]
23. Duncan D, Stupakoff A, Hedrick S, Marcu K, Siu G. *Mol. Cell. Biol*. 1995; 15:3179–3186. [PubMed: 7760814]
24. Parks C, Shenk T. *J. Virol*. 1997; 71:9600–9607. [PubMed: 9371624]
25. Salbaum J, Weidemann A, Lemaire H, Masters C, Beyreuther K. *EMBO J*. 1988; 7:2807–2 813. [PubMed: 3053167]
26. Mitsuda, N.; Boteva, K.; Gilbert, J.; Roses, A.; Vitek, M. Genbank Accession Number: AF029701. 1997.
27. Kim H, Kim Y, Nam J, Lee H, Rho H, Jung G. *Biochem. Biophys. Res. Comm*. 1994; 201:1526–1533. [PubMed: 8024598]
28. Ashfield R, Patel A, Bossone S, Brown H, Campbell R, Marcu K, Proudfoot N. *EMBO J*. 1994; 13:5656–5667. [PubMed: 7988563]
29. Komatsu M, Li H-O, Tsutsui H, Itakura K, Matsumura M, Yokoyama K. *Oncogene*. 1997; 15:1123–1131. [PubMed: 9294605]
30. Tsutsui H, Sakatsume O, Itakura K, Yokoyama K. *Biochem. Biophys. Res. Comm*. 1996; 226:801–809. [PubMed: 8831693]
31. Song J, Murakami J, Tsutsui H, Tang X, Matsumura M, Itakura K, Kanazawa I, Sun K, Yokoyama K. *J. Biol. Chem*. 1998; 273:20603–20694. [PubMed: 9685418]

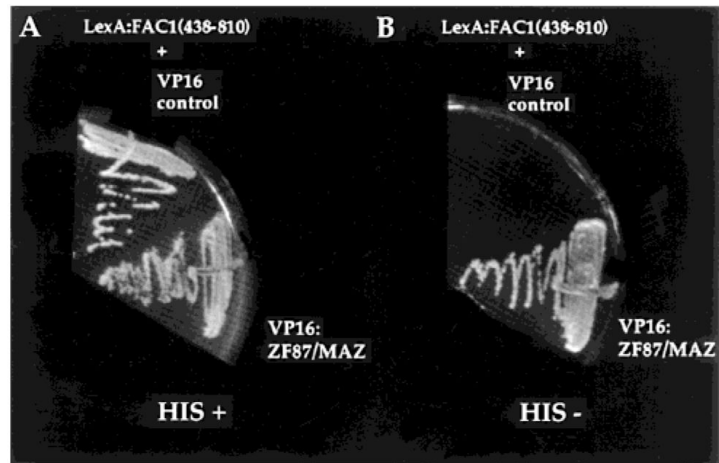


Figure 1.

FAC1 interacts with the myc-associated zinc finger protein (ZF87/MAZ) in yeast. Yeast colonies that were transformed with pLexA:FAC1(438–810) and pACT2 (VP16 alone) or pLexA: FAC1(438–810) and pACT2:ZF87/MAZ (VP16:ZF87/MAZ) were streaked on selective plates with (A) and without (B) the amino acid histidine.

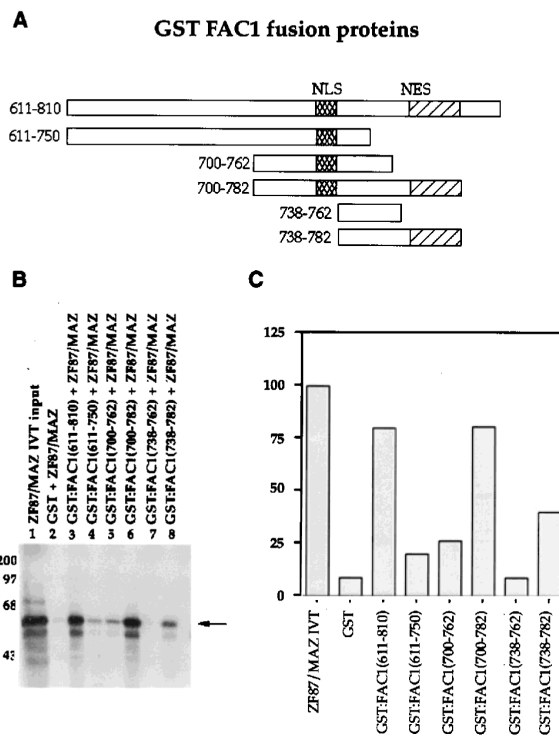


Figure 2. ZF87/MAZ interacts with the domain containing the putative nuclear localization sequence (NLS) and the nuclear export sequence (NES) of FAC1. (A) GST:FAC1 fusion proteins shown here were used to make affinity columns. In (B), ³⁵S-labeled in vitro translated ZF87/MAZ (lane 1) was added to the following affinity columns containing GST (lane 2), GST:FAC1(611–810) (lane 3), GST:FAC1(611–750) (lane 4), GST:FAC1(700–762) (lane 5), GST:FAC1(700–782) (lane 6), GST:FAC1(738–762) (lane 7), and GST:FAC1(738–782) (lane 8). Column-bound proteins were run on a 10% SDS-PAGE, which was transferred to nitrocellulose. The autoradiograph of the transferred gel is shown in B. The bound ZF87/MAZ was quantified using NIH image 1.5.8 and the results shown as a bar graph in (C).

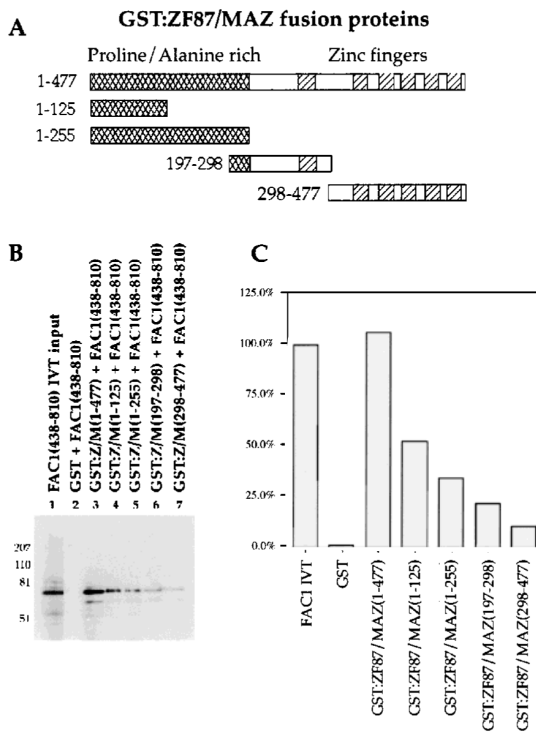


Figure 3. FAC1 interacts with ZF87/MAZ. The GST:MAZ fusion proteins produced to generate affinity columns are shown in (A). ³⁵S-labeled in vitro translated FAC1(438–810) (lane 1) was incubated with affinity columns containing the following proteins: GST (lane 2), GST:ZF87/MAZ(1–477) (lane 3), GST:ZF87/MAZ(1–125) (lane 4), GST:ZF87/MAZ(1–255) (lane 5), GST:ZF87/MAZ(197–298) (lane 6), and GST:ZF87/MAZ(298–477) (lane 7). Bound proteins were run on a 10% SDS-PAGE and transferred to nitrocellulose. Part (B) shows the autoradiograph of the transferred gel. The bound FAC1(438–810) was quantified using NIH image 1.5.8 and the results shown as a bar graph in (C).

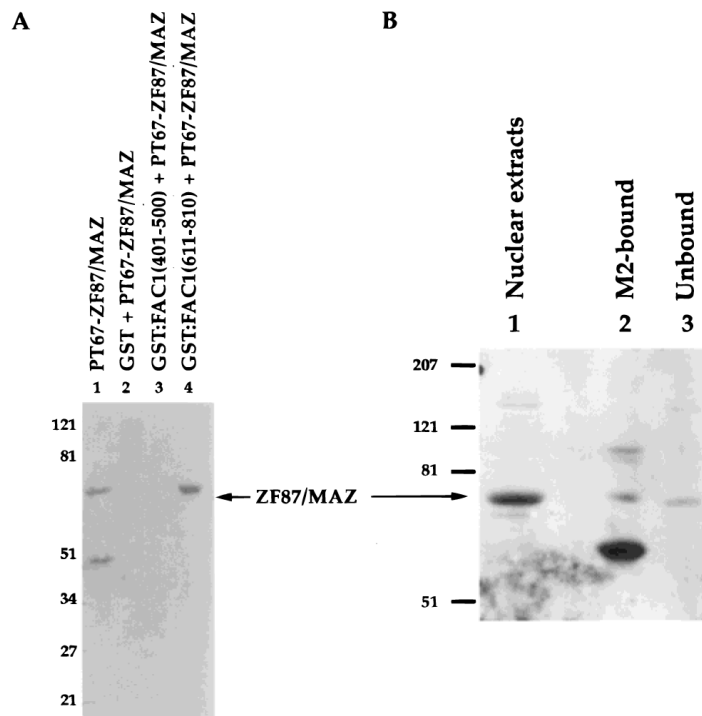
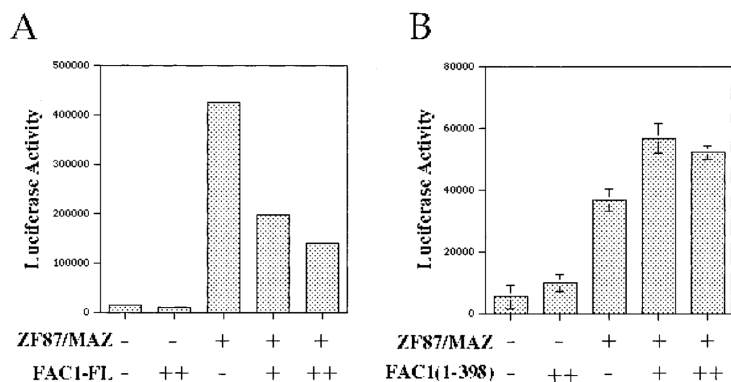
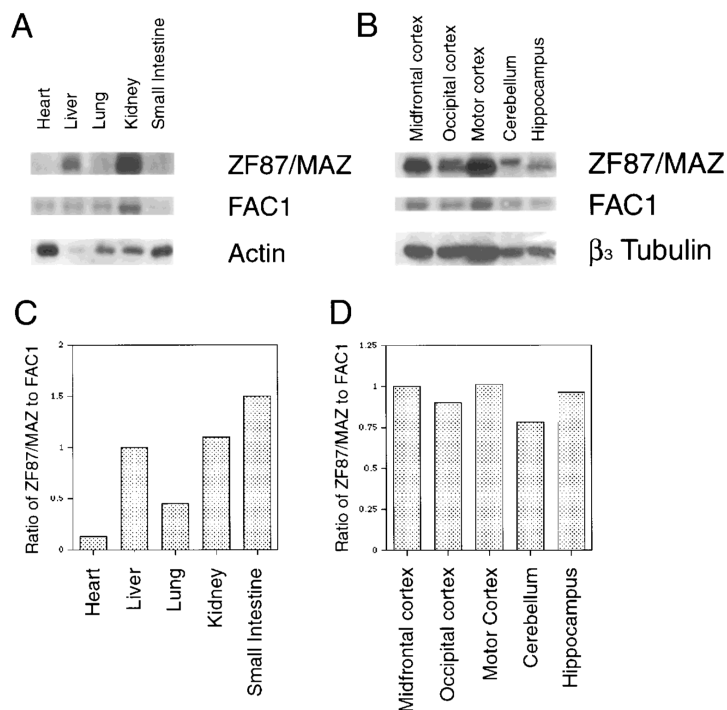


Figure 4.

In vivo produced ZF87/MAZ interacts with FAC1. (A) Nuclear extracts from cells transfected with epitope-tagged ZF87/MAZ cDNA were incubated with various GST:FAC1 affinity columns. Bound proteins were run on a 10% denaturing polyacrylamide gel, transferred to nitrocellulose, and immunoblotted for the epitope-tagged ZF87/MAZ. Shown is the immunoblot of: (1) 300 μ g of nuclear extract from ZF87/MAZ transfected PT67 cells, (2) eluate from GST column, (3) eluate from GST:FAC1(401–500) column, and (4) eluate from GST:FAC1(611–810) column. Again, the presence of the GST fusion proteins was verified by Ponceau S staining (data not shown). (B) Nuclear extracts from PT67 cells transfected with HA-tagged ZF87/MAZ and M2-tagged FAC1 (800 μ g) were incubated with M2-agarose beads as described in the Methods section under co-immunoprecipitation. Lane 1 is 300 μ g of nuclear extracts from transfected PT67 cells to demonstrate the abundance of the protein of interest in the starting material. Lane 2 contains the proteins bound to the M2 column. Lane 3 contains 1/4 of the unbound proteins present in the supernatant.

**Figure 5.**

FAC1 reduces transcriptional activation of the SV40 promoter by ZF87/MAZ. (A) NIH3T3 cells were transfected with 4 μg of reporter vector, pGL-2 control (Promega), which contains the SV40 promoter and enhancer elements (SV40). The reporter construct was introduced by itself (– –), with 0.6 μg pcDNA3.1 FAC1-FL (++ FAC1-FL) by itself, with 0.5 μg pcDNA3.1-ZF87/MAZ (+ ZF87/MAZ) by itself or in combination with 0.3 μg pcDNA3.1-FAC1 (+ FAC1), or with 0.6 μg pcDNA3.1-FAC1 (++ FAC1). (B) pGL-2 control was cotransfected into NIH3T3 cells with a FAC1 mutant lacking the carboxy terminal domain required for ZF87/MAZ interaction (FAC1(1–398)). The reporter was transfected by itself (– –), with 0.6 μg pcDNA3.1-FAC1(1–398) by itself (++ FAC1(1–398)), with 0.5 μg pcDNA3.1-ZF87/MAZ (+ ZF87/MAZ) by itself or in combination with 0.3 μg of pcDNA3.1-FAC1(1–398) (+FAC1(1–398)) or 0.6 μg of pcDNA3.1-FAC1(1–398) (++ FAC1(1–398)). The pcDNA3.1 vector was included in reactions to keep the amount of expression vector constant in all reactions. The values shown in A and B are the average luciferase activity from three experiments corrected for protein concentration. The error bars denote the standard deviation. Some of these are so small as not to be seen on the graph at the current scale (<1%).

**Figure 6.**

ZF87/MAZ and FAC1 exhibit similar relative expression levels in various tissues. Protein extracts from various tissues and brain regions were fractionated by size on an 8% SDS-PAGE. 125 μg of each sample was loaded in the following order: (A) heart, liver, lung, kidney, and small intestine; (B) midfrontal cortex, occipital cortex, motor cortex, cerebellum, and hippocampus. After electroblotting, membranes were probed with anti-ZF87/MAZ antibody. The blots were stripped and re-probed with anti-FAC1 antibody. The multiple tissue blot (A) was stripped and re-probed with anti-actin antibody, and the multiple brain regions blot (B) was re-probed with anti- β_3 tubulin antibody as controls for loading. Bands in each lane were quantitated and normalized to the loading control. The ratio of ZF87/MAZ:FAC1 for each tissue is shown in C.

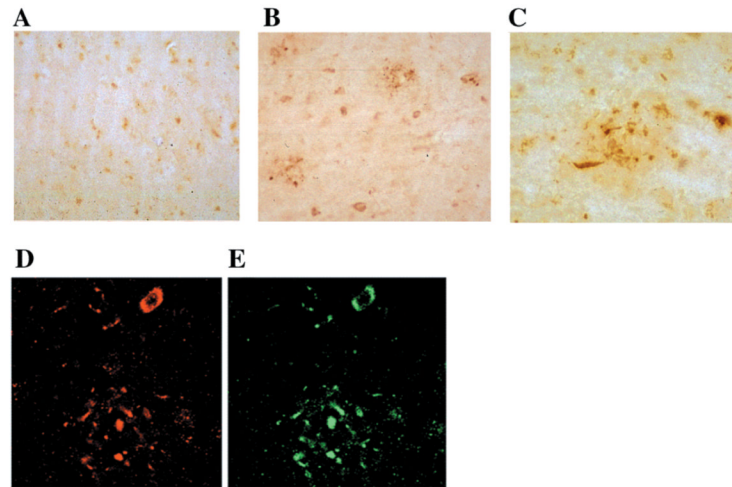


Figure 7.

ZF87/MAZ co-localizes with FAC1 in β -amyloid containing plaques. Midfrontal cortex of an age-matched, normal individual (A, 20X) and an individual with Alzheimer's disease (B, 20X) stains positively for ZF87/MAZ by immunocytochemistry. Close up of ZF87/MAZ positive β -amyloid plaque is shown in C (40X). Co-localization between FAC1 (D) and ZF87/MAZ (E) is demonstrated by double label immunofluorescent laser confocal microscopy. FAC1 is visualized using a Cy5 conjugated secondary antibody. ZF87/MAZ is stained with a FITC conjugated secondary antibody. D and E contain a β -amyloid plaque, which labels positively for both FAC1 and ZF87/MAZ.